Article

Tuning the Absorption, Charge Transport Properties, and Solar Cell Efficiency with the Number of Thienyl Rings in Platinum-Containing Poly(aryleneethynylene)s

Wai-Yeung Wong, Xing-Zhu Wang, Ze He, Kwok-Kwan Chan, Aleksandra B. Djurii, Kai-Yin Cheung, Cho-Tung Yip, Alan Man-Ching Ng, Yan Yan Xi, Chris S. K. Mak, and Wai-Kin Chan

J. Am. Chem. Soc., **2007**, 129 (46), 14372-14380• DOI: 10.1021/ja074959z • Publication Date (Web): 30 October 2007

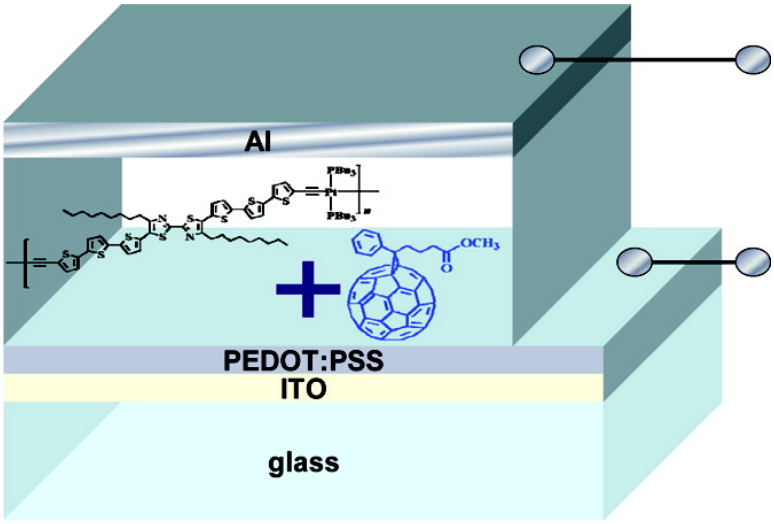

More About This Article

Additional resources and features associated with this article are available within the HTML version:

- Supporting Information
- Links to the 14 articles that cite this article, as of the time of this article download
- Access to high resolution figures
- Links to articles and content related to this article
- Copyright permission to reproduce figures and/or text from this article

View the Full Text HTML

J|A|C|S
ARTICLES
Published on Web 10/30/2007

Tuning the Absorption, Charge Transport Properties, and Solar Cell Efficiency with the Number of Thienyl Rings in Platinum-Containing Poly(aryleneethynylene)s

Wai-Yeung Wong,*[,†] Xing-Zhu Wang,[†,‡] Ze He,[†] Kwok-Kwan Chan,[†] Aleksandra B. Djurišić,*[,§] Kai-Yin Cheung,[§] Cho-Tung Yip,[§] Alan Man-Ching Ng,[§] Yan Yan Xi,[§] Chris S. K. Mak,[||] and Wai-Kin Chan[||]

Contribution from the Department of Chemistry and Centre for Advanced Luminescence Materials, Hong Kong Baptist University, Waterloo Road, Kowloon Tong, Hong Kong, P. R. China, Key Laboratory of Environmentally Friendly Chemistry and Applications of Ministry of Education, College of Chemistry, Xiangtan University, Xiangtan 411105, Hunan Province, P. R. China, and Departments of Chemistry and Physics, The University of Hong Kong, Pokfulam Road, Hong Kong, P. R. China

Received July 5, 2007; E-mail: rwywong@hkbu.edu.hk; dalek@hkusua.hku.hk

Abstract: The synthesis, characterization, and photophysics of a series of solution-processable and strongly visible-light absorbing platinum(II) polyynes containing bithiazole-oligo(thienyl) rings were presented. Tuning the polymer solar cell efficiency, as well as optical and charge transport properties, in soluble, low-band gap Pt^{II}-based conjugated poly(heteroaryleneethynylene)s using the number of oligothienyl rings is described. These materials are highly soluble in polar organic solvents due to the presence of solubilizing bithiazole moieties and show strong absorptions in the solar spectra, rendering them excellent candidates for bulk heterojunction polymer solar cells. Their photovoltaic responses and power conversion efficiencies (PCEs) depend to a large extent on the number of thienyl rings along the main chain, and some of them can be used to fabricate highly efficient solar cells with PCEs of up to 2.7% and a peak external quantum efficiency to 83% under AM1.5 simulated solar illumination, which is comparable to that of poly(3-hexylthiophene)-based devices fabricated without additional processing (annealing or TiO_x layer). The influence of the number of thienyl rings and the metal group on the performance parameters and optimization of solar cell efficiency was evaluated and discussed in detail. At the same blend ratio of 1:4, the light-harvesting ability and PCE increase sharply as the thienyl chain length increases. The present work provides an attractive approach to developing conjugated metallopolymers offering broad solar absorptions and tunable solar cell efficiency and demonstrates the potential of metalated conjugated polymers for efficient power generation.

Introduction

Harvesting energy directly from sunlight using photovoltaic technology is increasingly recognized as a solution to the world's energy problem.[1] Solar cells based on solution-processable organic semiconducting polymers have attracted considerable interest as a low-cost alternative to inorganic semiconductors for large-area and lightweight applications.[2] While excellent performance (5−6% efficiency) has been reported for solar cells based on bulk heterojunctions consisting of poly(3-hexylthiophene) (P3HT) as a donor material and [6,6]-phenyl-C_{61}-butyric acid methyl ester (PCBM) as an acceptor material,[3] it has been recognized that novel materials need to be developed in order to obtain solar cells with an efficiency exceeding 10% (threshold for commercial applications).[4] So, efforts have been made for designing better materials to improve coverage of the solar spectrum and hence enhance the efficiency of polymer photovoltaic cells by extending the absorption to longer wavelengths, increasing the absorption coefficients (ϵ_{max}), and optimizing the charge transport properties for forming efficient blends with fullerenes in bulk heterojunction cells.[3a,h,4]

† Hong Kong Baptist University.
‡ Xiangtan University.
§ Department of Physics, The University of Hong Kong.
|| Department of Chemistry, The University of Hong Kong.

(1) (a) Shaheen, S. E.; Ginley, D. S.; Jabbour, G. E. *MRS Bull.* **2005**, *30*, 10. (b) Barnham, K. W. J.; Mazzer, M.; Clive, B. *Nature* **2006**, *5*, 161.
(2) (a) Brabec, C. J.; Sariciftci, N. S.; Hummelen, J. C. *Adv. Funct. Mater.* **2001**, *11*, 15. (b) Coakley, K. M.; McGehee, M. D. *Chem. Mater.* **2004**, *16*, 4533. (c) Günes, S.; Neugebauer, H.; Sariciftci, N. S. *Chem. Rev.* **2007**, *107*, 1324. (d) Winder, C.; Saricftci, N. S. *J. Mater. Chem.* **2004**, *14*, 1077.
(3) (a) Kim, J. Y.; Kim, S. H.; Lee, H. H.; Lee, K.; Ma, W.; Gong, X.; Heeger, A. J. *Adv. Mater.* **2006**, *18*, 572. (b) Reyes-Reyes, M.; Kim, K.; Carroll, D. J. *Appl. Phys. Lett.* **2005**, *87*, 083506. (c) Kim, Y.; Cook, S.; Tuladhar, S. M.; Choulis, S. A.; Nelson, J.; Durrant, J. R.; Bradley, D. D. C.; Giles, M.; McCulloch, I.; Ha, C. S.; Ree, M. *Nat. Mater.* **2006**, *5*, 197. (d) Li, G.; Shrotriya, V.; Huang, J.; Yao, Y.; Moriarty, T.; Emery, K.; Yang, Y. *Nat. Mater.* **2005**, *4*, 864. (e) Li, G.; Shortriya, V.; Yao, Y.; Yang, Y. *J. Appl. Phys.* **2005**, *98*, 043704. (f) Kim, Y.; Choulis, S. A.; Nelson, J.; Bradley, D. D. C.; Cook, S.; Durrant, J. R. *Appl. Phys. Lett.* **2006**, *86*, 063502. (g) De Bettignies, R.; Leroy, J.; Firon, M.; Sentein, C. *Synth. Met.* **2006**, *156*, 510. (h) Mihailetchi, V. D.; Xie, H.; de Boer, B.; Popescu, L. M.; Hummelen, J. C.; Blom, P. W. M.; Koster, L. J. A. *Appl. Phys. Lett.* **2006**, *89*, 012107. (i) von Hauff, E.; Parisi, J.; Dyakonov, V. *J. Appl. Phys.* **2006**, *100*, 043702−1. (j) Kim, K.; Liu, J.; Namboothiry, M. A. G.; Carroll, D. L. *Appl. Phys. Lett.* **2007**, *90*, 163511.
(4) (a) Koster, L. J. A.; Mihailetchi, V. D.; Bloom, P. W. *Appl. Phys. Lett.* **2006**, *88*, 093511. (b) Scharber, M. C.; Mühlbacher, D.; Koppe, M.; Denk, P.; Waldauf, C.; Heeger, A. J.; Brabec, C. J. *Adv. Mater.* **2006**, *18*, 789. (c) Peet, J.; Kim, J. Y.; Coates, N. E.; Ma, W. L.; Moses, D.; Heeger, A. J.; Bazan, G. C. *Nat. Mater.* **2007**, *6*, 497.

 10.1021/ja074959z CCC: $37.00

However, although several organic polymers with lower band gaps than P3HT have been reported, the achieved power conversion efficiency (PCE) was typically lower compared to the best achieved results for P3HT based cells.[5] Typically, the efficiency of low band gap polymer based solar cells is in the range ~2.2−3.2%,[5a−e] while efficiencies exceeding 4−5% have been only recently reported.[5f,g] It should be noted that most of the efforts in developing new materials are focused on novel donor materials[5] and establishing what properties a desirable donor material should have in order to result in efficient solar cells based on a bulk heterojunction with PCBM.[4b] An alternative method for improving device performance could be placed on changing the acceptor material, since it has been proposed that lowering of the LUMO level of the acceptor would be more beneficial to the cell performance than lowering the band gap of the polymer.[4a] However, although efficient cells with other acceptor molecules have been demonstrated,[6] the majority of polymer solar cells are based on a PCBM acceptor. Nevertheless, a recent report that a polyfluorene based polymer yields similar efficiency in bulk heterojunctions with P3HT and PCBM[6a] highlights the need for expanding the flexibility of solar cell designs to include a greater variety of functional materials. However, due to the large number of possible material combinations, and with each new material requiring optimization of cell fabrication conditions to achieve good results, this would be a very difficult task and inevitably most of the novel donor polymer design efforts are focused on donors which would be combined with PCBM. One possible solution to this problem would be to develop a new class of polymers with easily tunable properties which can be solution-processed under similar conditions.

Metal-containing conjugated organic polymers represent an intriguing and promising class of materials,[7] and platinum alkynyls have been a popular candidate for inclusion into such a polymeric backbone.[8] While organometallic donor materials are widely used in small-molecule solar cells,[9] soluble π-conjugated organometallic polyynes were much less explored and, in most cases, the efficiency was low due to low coverage in the solar spectral region,[8a,e,f,h] although there can be an involvement of a triplet state for energy conversion.[8f,h] We have recently demonstrated efficient solar cells based on platinum metallopolyyne/PCBM bulk heterojunctions.[5f] While further improvements in the achieved solar cell efficiency are expected with optimization of the processing conditions and device architecture, a design limit will eventually be reached, as determined by the charge mobilities and energy levels of the material. For greater flexibility in the solar cell design, a class of polymers with tunable functional properties is desirable. Here we report some strongly visible-absorbing and band gap tunable metalated conjugated polymers with the unexplored bis(oligothienyl)-2,2′-bithiazole donor−acceptor (D−A) hybrid spacers, and solar cells derived from them showed high PCEs of up to 2.7%. The work allows an effective tuning of PCE by simple tailoring of the number of thienyl rings, which changes the absorption features and charge carrier mobilities of the resulting metallopolymers.

Results and Discussion

Synthetic Strategies and Chemical Characterization. The chemical structures of new platinum(II) polyyne polymers **P0**−**P3** and their well-defined model compounds **M0**−**M3** are shown in Scheme 1. The dibromo precursors (**L1-2Br**, **L2-2Br**, and **L3-2Br**) can be obtained from **L0-2Br** by successive coupling of the 2-thienylmagnesium bromide with the corresponding dibromide of the lower generation. Conversion of the dibromide derivatives to their corresponding diethynyl congeners can be readily achieved following the typical organic synthetic protocols for alkynylation of aromatic halides.[8b,d,u] The Pt compounds were prepared by the Sonogashira-type dehydrohalogenation reaction between each of **L0**−**L3** and the platinum chloride precursors.[8j] The use of long nonyl chains on bithiazole is crucial in increasing the solubility and improving the solution processability/tractability of these metallopolymers. The polymers can be purified by silica column chromatography and repeated precipitation and isolated in good yield and high purity. All these Pt compounds are thermally and air stable and soluble in common chlorinated hydrocarbons and toluene. **P0**−**P3** can cast tough, free-standing thin films from their solutions readily, but their solubility tends to decrease gradually as *m* increases. Gel-

(5) (a) Zhou, Q.; Hou, Q.; Zheng, L.; Deng, X.; Yu, G.; Cao, Y. *Appl. Phys. Lett.* **2004**, *84*, 1653. (b) Svensson, M.; Zhang, F.; Veenstra, S. C.; Verhees, W. J. H.; Hummelen, J. C.; Kroon, J. M.; Inganäs, O.; Anderson, M. R. *Adv. Mater.* **2003**, *15*, 988. (c) Zhang, F.; Mammo, W.; Andersson, L. M.; Admassie, S.; Andersson, M. R.; Inganäs, O. *Adv. Mater.* **2006**, *18*, 2169. (d) Hou, J.; Tan, Z.; Yan, Y.; He, Y.; Yang, C.; Li, Y. *J. Am. Chem. Soc.* **2006**, *128*, 4911. (e) Mühlbacher, D.; Scharber, M.; Morana, M.; Zhu, Z.; Waller, D.; Gaudiana, R.; Brabec, C. *Adv. Mater.* **2006**, *18*, 2884. (f) Wong, W.-Y.; Wang, X.-Z.; He, Z.; Djurišić, A. B.; Yip, C.-T.; Cheung, K.-Y.; Wang, H.; Mak, C. S.-K.; Chan, W.-K. *Nat. Mater.* **2007**, *6*, 521. (g) Peet, J.; Kim, J. Y.; Coates, N. E.; Ma, W. L.; Moses, D.; Heeger, A. J.; Bazan, G. C. *Nat. Mater.* **2007**, *6*, 497.

(6) (a) McNeill, C. R.; Abrusci, A.; Zaumsell, J.; Wilson, R.; McKiernan, M. J.; Burroughes, J. H.; Halls, J. J. M.; Greenham, N. C.; Friend, R. H. *Appl. Phys. Lett.* **2007**, *90*, 193506. (b) Yao, Y.; Shi, C.; Li, G.; Shotriya, V.; Pei, Q.; Yang, Y. *Appl. Phys. Lett.* **2006**, *89*, 153507. (c) Alam, M. M.; Jenekhe, S. A. *Chem. Mater.* **2004**, *16*, 4647.

(7) (a) Manners, I. *Science* **2001**, *294*, 1664. (b) Nguyen, P.; Gómez-Elipe, P.; Manners, I. *Chem. Rev.* **1999**, *99*, 1515. (c) Kingsborough, R. P.; Swager, T. M. *Prog. Inorg. Chem.* **1999**, *48*, 123. (d) Abd-El-Aziz, A. S. *Macromol. Rapid Commun.* **2002**, *23*, 995. (e) Holliday, B. J.; Swager, T. M. *Chem. Commun.* **2005**, 23. (f) Fustin, C.-A.; Guillet, P.; Schubert, U. S.; Gohy, J.-F. *Adv. Mater.* **2007**, *19*, 1665. (g) Abd-El-Aziz, A. S.; Todd, E. K. *Coord. Chem. Rev.* **2003**, *246*, 3. (h) Abd-El-Aziz, A. S.; Carraher, C. E., Jr.; Pittman, C. U., Jr.; Zeldin, M. *Macromolecules Containing Metal and Metal-Like Elements*; Wiley-Interscience: New Jersey, 2005; Vol. 5. (i) Wolf, M. O. *J. Inorg. Organomet. Polym. Mater.* **2006**, *16*, 189. (j) Abd-El-Aziz, A. S., Manners, I., Eds. *Frontiers in Transition Metal-Containing Polymers*; Wiley-Interscience: New Jersey, 2007. (k) Fyfe, H. B.; Mlekuz, M.; Zargarian, D.; Taylor, N. J.; Marder, T. B. *J. Chem. Soc., Chem. Commun.* **1991**, 188.

(8) (a) Younus, M.; Köhler, A.; Cron, S.; Chawdhury, N.; Al-Mandhary, M. R. A.; Khan, M. S.; Lewis, J.; Long, N. J.; Friend, R. H.; Raithby, P. R. *Angew. Chem., Int. Ed.* **1998**, *37*, 3036. (b) Long, N. J.; Williams, C. K. *Angew. Chem., Int. Ed.* **2003**, *42*, 2586. (c) Manners, I. *Synthetic Metal-Containing Polymers*; Wiley-VCH: Weinheim, 2004. (d) Wong, W.-Y.; Ho, C.-L. *Coord. Chem. Rev.* **2006**, *250*, 2627. (e) Chawdhury, N.; Köhler, A.; Friend, R. H.; Wong, W.-Y.; Lewis, J.; Younus, M.; Raithby, P. R.; Corcoran, T. C.; Al-Mandhary, M. R. A.; Khan, M. S. *J. Chem. Phys.* **1999**, *110*, 4963. (f) Guo, F.; Kim, Y. G.; Reynolds, J. R.; Schanze, K. S. *Chem. Commun.* **2006**, 1887. (g) Silverman, E. E.; Cardolaccia, T.; Zhao, X.; Kim, K. Y.; Haskins-Glusac, K.; Schanze, K. S. *Coord. Chem. Rev.* **2005**, *249*, 1491. (h) Köhler, A.; Wittman, H. F.; Friend, R. H.; Khan, M. S.; Lewis, J. *Synth. Met.* **1996**, *77*, 147. (i) Wong, W.-Y. *Comment Inorg. Chem.* **2005**, *26*, 39. (j) Wong, W.-Y. *J. Inorg. Organomet. Polym. Mater.* **2005**, *15*, 197. (k) Yam, V. W.-W. *Acc. Chem. Res.* **2002**, *35*, 555. (l) Szafert, S.; Gladysz, J. A. *Chem. Rev.* **2003**, *103*, 4175. (m) Powell, C. E.; Humphrey, M. G. *Coord. Chem. Rev.* **2004**, *248*, 725. (n) Bruce, M. I.; Low, P. J. *Adv. Organomet. Chem.* **2004**, *50*, 179. (o) Uwe, U. H. F. *Chem. Rev.* **2000**, *100*, 1605. (p) Davies, S. J.; Johnson, B. F. G.; Khan, M. S.; Lewis, J. *J. Chem. Soc., Chem. Commun.* **1991**, 187. (q) Lewis, J.; Khan, M. S.; Johnson, B. F. G.; Marder, T. B.; Fyfe, H. B.; Wittmann, F.; Friend, R. H.; Dray, A. E. *J. Organomet. Chem.* **1992**, *425*, 165. (r) Fujikura, Y.; Sonogashira, K.; Hagihara, N. *Chem. Lett.* **1975**, 1067. (s) Sonogashira, K.; Takahashi, S.; Hagihara, N. *Macromolecules* **1977**, *10*, 879. (t) Sonogashira, K.; Kataoka, S.; Takahashi, S.; Hagihara, N. *J. Organomet. Chem.* **1978**, *160*, 319. (u) Takahashi, S.; Kuroyama, Y.; Sonogashira, K.; Hagihara, N. *Synthesis* **1980**, 627.

(9) (a) Xue, J.; Uchida, S.; Rand, B. P.; Forrest, S. R. *Appl. Phys. Lett.* **2004**, *84*, 3013. (b) Robertson, N. *Angew. Chem., Int. Ed.* **2006**, *45*, 2338. (c) Reagan, D. O.; Grätzel, M. *Nature* **1991**, *353*, 737. (d) Grätzel, M. *Inorg. Chem.* **2005**, *44*, 6841.

Scheme 1. Synthetic Pathways to Bithiazole-Oligo(thiophene) Based Ligand Precursors and Their Platinum Compounds[a]

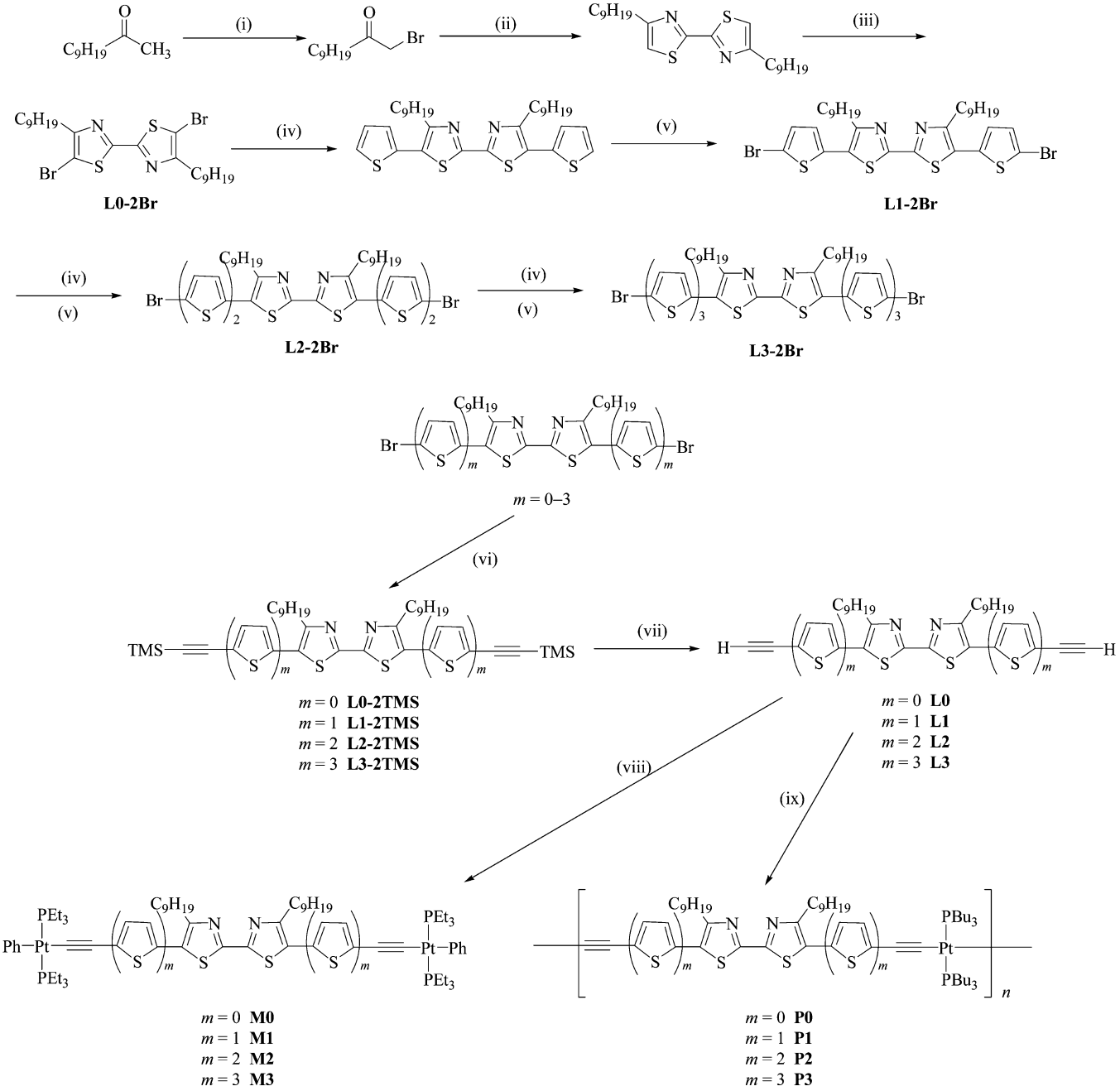

[a] Conditions and reagents: (i) Br_2, H_2SO_4/H_2O; (ii) dithiooxamide, EtOH; (iii) NBS, DMF/AcOH; (iv) 2-thienylmagnesium bromide, $Pd(dppf)Cl_2$, THF; (v) NBS, $CHCl_3$/AcOH; (vi) $Me_3SiC{\equiv}CH$, $Pd(OAc)_2$, PPh_3, CuI, Et_3N; (vii) K_2CO_3, $MeOH/CH_2Cl_2$; (viii) *trans*-$[PtPh(Cl)(PEt_3)_2]$, CuI, Et_3N; (ix) *trans*-$[Pt(n\text{-}Bu_3P)_2Cl_2]$, CuI, Et_3N.

permeation chromatography on **P0**−**P3** suggests a high-molecular-weight material with the degree of polymerization ∼10−34 (∼56−80 heterocyclic rings in total) (Table 1). The structures were unequivocally characterized using elemental analyses, mass spectrometry, and IR and NMR spectroscopies (see Supporting Information). To our knowledge, **P3** represents a soluble metal polyyne consisting of up to eight heterocycles in the repeat unit.

Photophysical and Electrochemical Characterization. The absorption and emission spectra of the polymers and model complexes were measured in CH_2Cl_2 solutions at 293 K (Figure 1). The absorption of **P0**−**P3** is each dominated by an intense band peaking at 452−481 nm, and these polymers can emit strong fluorescence from the singlet excited states at 497−603 nm. The absorption and emission properties of **M0**−**M3** are very similar to those of **P0**−**P3**, with the absorption maxima in

Table 1. Photophysical Data of **P0**−**P3**

polymer	M_w[a]	M_n[b]	DP[c]	T_{dec}[d] [°C]	λ_{abs} in CH_2Cl_2 [nm]	λ_{em}[e] in CH_2Cl_2 [nm]
P0	67 930	35 570	34	355	452, 474	497 (6.4, 1.93)
P1	29 850	17 350	14	352	346, 468	557 (5.7, 1.16)
P2	36 060	17 590	13	359	378,[f] 476	592 (5.1, 1.34)
P3	28 740	15 700	10	363	397,[f] 481	603 (3.2, 0.85)

[a] Weight-average molecular weight. [b] Number-average molecular weight. [c] Degree of polymerization. [d] Onset decomposition temperature. [e] Quantum yields and lifetimes in ns (Φ, τ) are shown in parentheses. [f] Shoulder peak.

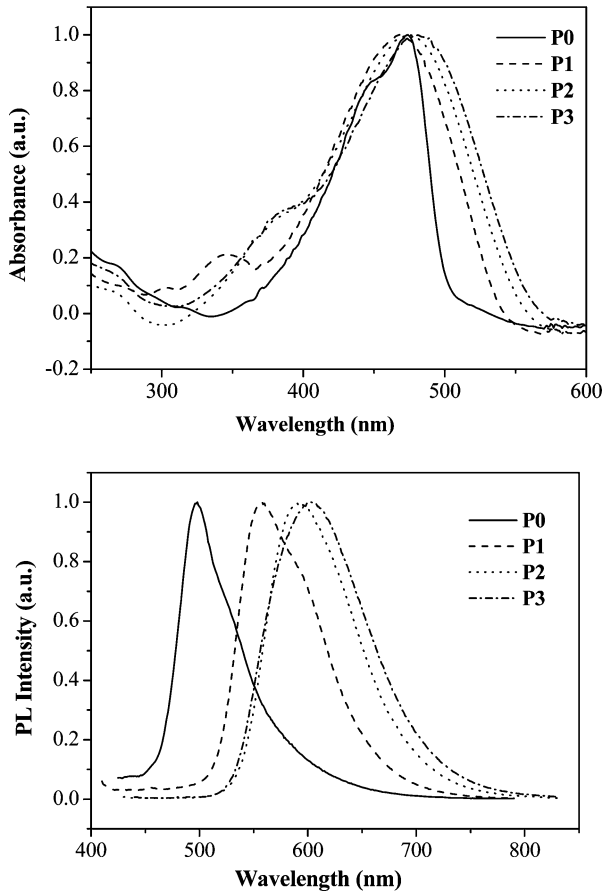

Figure 1. Absorption and PL spectra of **P0**−**P3** in CH_2Cl_2 at 293 K (concn ca. 10^{-5} M).

the range 437−473 nm. Due to the presence of a more extended π-electron delocalized system through the rigid chain and the creation of an alternate D−A chromophore[10] based on a highly electron-accepting bithiazole ring (*n*-doping)[11] in combination with the electron-donating thiophene rings (*p*-doping),[12] the band gaps of **P0**−**P3** vary from 2.40 to 2.06 eV with the value for red **P3** being significantly reduced by ca. 0.34 eV relative to the yellow **P0**. If the D and A moieties are separated by neutral parts and extended through the Pt and alkynyl units, we can get a smaller band gap, typical of the inorganic n-i-p-i superlattice quantum well structures.[10d] However, the extent of red shifts induced by increasing *m* is less pronounced, and there would be little benefit in extending the π-conjugation by increasing *m* above 7 or 8 (see Supporting Information). A linear oligothienyl chain length dependence of E_g can be rationalized from the plot of E_g against reciprocal chain length, and a limiting

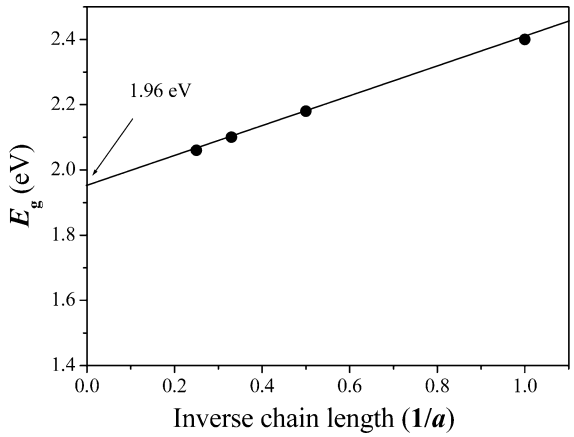

Figure 2. Relationship of E_g and $1/a$ ($a = m + 1$) for **P0**−**P3**.

value for E_g is estimated to be ca. 1.96 eV for $m = \infty$ (Figure 2).[13] The measured photoluminescence lifetimes for **P0**−**P3** and **M0**−**M3** are all very short (ca. 0.85−2.22 ns), characteristic of the spin-allowed singlet emission. These results and the small Stokes shift preclude the emitting state as a triplet but a singlet excited state instead.[8a,d] We observed no emission from a triplet excited state over the measured spectral window between 1.2 and 3.1 eV for **P0**−**P3**. This is in accordance with the energy gap law for Pt-containing conjugated polyynes and their model diynes,[14] and a tradeoff problem between the band gap and the phosphorescence decay rate exists in such a metallayne system. The nonradiative decay rate $(k_{nr})_P$ from the triplet state increases exponentially with the decreasing triplet−singlet energy gap according to the expression $(k_{nr})_P \propto \exp(-C\Delta E_{S-T})$, where ΔE_{S-T} is the energy gap for the T_1-S_0 transition and *C* is a term controlled by the molecular parameters and vibrational modes.[14] Hence, a high band gap polymer will likely be phosphorescent, whereas a low band gap value will be detrimental for the triplet emission. In addition, the highly extended heteroaryl rings in the ligand reduces largely the influence of heavy metal which is mainly responsible for the intersystem crossing and thus phosphorescence. Therefore, it is not the triplet state but mostly a charge-transfer (CT) excited state that contributes to the efficient photoinduced charge separation in the energy conversion for **P0**−**P3**,[5f,8a] which is different from the Pt-monothiophene polyyne-based blends where charge separation occurs via the triplet state of the polymer.[8f] From these results, we attribute the localized states centered at 2.06−2.50 eV to a strong CT-type interaction for the polymers. The CT nature of the transition was also manifested by the solvent dependent emission spectra of these Pt polyynes. For instance, **P3** exhibited a positive solvatochromism with a red shift of the peak maximum of ~52 nm from toluene (λ_{em} = 566 nm) to CH_2Cl_2 (λ_{em} = 618 nm), which suggests a more polar excited state. Likewise, the PL spectra of **P2** are solvatochromic (λ_{em} = 539 in toluene and 563 nm in CH_2Cl_2). We think that the D−A interaction along the bithiazole-oligothienyl unit is remarkably enhanced by the extensive π-delocalization in the polymer backbone containing the electron-rich Pt ion. This gives

(10) (a) Roncali, J. *Chem. Rev.* **1997**, *97*, 173. (b) Wong, W.-Y.; Choi, K.-H.; Lu, G.-L.; Shi, J.-X. *Macromol. Rapid Commun.* **2001**, *22*, 461. (c) Köhler, A.; Younus, M.; Al-Mandhary, M. R. A.; Raithby, P. R.; Khan, M. S.; Friend, R. H. *Synth. Met.* **1999**, *101*, 246. (d) Havinga, E. E.; Haeve, W.; Wynberg, H. *Synth. Met.* **1993**, *55-57*, 299.

(11) (a) Yamamoto, T.; Suganuma, H.; Maruyama, T.; Inoue, T.; Muramatsu, Y.; Arai, M.; Komarudin, D.; Ooba, N.; Tomaru, S.; Sasaki, S.; Kubota, K. *Chem. Mater.* **1997**, *9*, 1217. (b) Cao, J.; Kampf, J. W.; Curtis, M. D. *Chem. Mater.* **2003**, *15*, 404. (c) MacLean, B. J.; Pickup, P. G. *J. Mater. Chem.* **2001**, *11*, 1357. (d) Politis, J. K.; Curtis, M. D.; Gonzalez, L.; Martin, D. C.; He, Y.; Kanicki, J. *Chem. Mater.* **1998**, *10*, 1713. (e) Masui, K.; Mori, A.; Okano, K.; Takamura, K.; Kinoshita, M.; Ikeda, T. *Org. Lett.* **2004**, *6*, 2011.

(12) (a) Perepichka, I. F.; Perepichka, D. F.; Meng, H.; Wudl, F. *Adv. Mater.* **2005**, *17*, 2281. (b) McCullough, R. D. *Adv. Mater.* **2005**, *17*, 2281. (c) Fichou, D., Ed. *Handbook of Oligo- and Polythiophenes*; Wiley-VCH: New York, 1999. (d) Roncali, J.; Blanchard, P.; Frère, P. *J. Mater. Chem.* **2005**, *15*, 1589. (e) Stott, T. L.; Wolf, M. O. *Coord. Chem. Rev.* **2003**, *246*, 89.

(13) (a) Zade, S. S.; Bendikov, M. *Org. Lett.* **2006**, *8*, 5243. (b) Bäuerle, P. *Adv. Mater.* **1992**, *4*, 102. (c) Lahti, P. M.; Obrzut, J.; Karasz, F. E. *Macromolecules* **1987**, *20*, 2023.

(14) Wilson, J. S.; Chawdhury, N.; Al-Mandhary, M. R. A.; Younus, M.; Khan, M. S.; Raithby, P. R.; Köhler, A.; Friend, R. H. *J. Am. Chem. Soc.* **2001**, *123*, 9412.

Table 2. Physical Data and Photovoltaic Performance of **P0**−**P3**; the Photovoltaic Performance Parameters Represent an Average from 5 to 20 Devices

polymer	E_g[a] [eV]	E_{ox} [V]	E_{HOMO} [eV]	E_{LUMO}[b] [eV]	V_{oc} [V]	I_{sc} [mA cm^{-2}]	*FF*	PCE [%]
P0	2.40 (2.46)	0.84	−5.91	−3.51	0.73	0.91 (0.79)[d]	0.32	0.21
P1	2.18 (2.28)	0.75	−5.82	−3.64	0.83	2.33 (1.63)[d]	0.39	0.76
P2	2.10 (2.22)	0.70	−5.79	−3.69	0.81 (0.90)[c]	6.93 (6.39)[c] (5.88)[d]	0.38 (0.46)[c]	2.14 (2.66)[c]
P3	2.06 (2.19)	0.31	−5.71	−3.65	0.88 (0.88)[c]	6.50 (6.01)[c] (4.70)[d]	0.44 (0.43)[c]	2.50 (2.30)[c]

[a] Optical bandgaps determined from onset of absorption in solid state. The corresponding values obtained from the solution phases are shown in parentheses. [b] Calculated from $E_{HOMO} + E_g$. [c] At **P2** or **P3**/PCBM (1:5, w/w) ratio. [d] I_{sc} values estimated from the integration of EQE spectrum under theoretical AM1.5 global irradiation.

rise to a CT-type transition that causes a substantial lowering of the optical gap.

Cyclic voltammetry of the films for **P0**−**P3** was performed (Table 2). **P0**−**P3** show an irreversible thienyl oxidation at 0.84, 0.75, 0.70, and 0.31 V, respectively, which agrees with the phenomenon that formation of the heteroaromatic cation radicals is favored by increased conjugation length.[15] The electrooxidation of oligothiophenes is often irreversible because the electrogenerated cations readily undergo rapid coupling reactions leading to higher oligomers or polymers. The stability of these radical cations increases when *m* becomes longer.[15] Hence, the HOMO levels tend to be elevated with increasing *m* from **P0** to **P3**.

Polymer Photovoltaic Behavior. Polymer solar cells were fabricated by using each of **P0**−**P3** as an electron donor and PCBM as an electron acceptor (Table 2). The hole collection electrode consisted of indium tin oxide (ITO) with a spin-coated poly(3,4-ethylene-dioxythiophene):poly(styrene sulfonate) (PEDOT:PSS), while Al served as the electron collecting electrode. It can be clearly observed that enhancing the absorption coefficient of the band by increasing the conjugation length of the chain with oligothienyl rings is a good strategy. The facile functionalization of thiophene groups also offers relatively efficient synthetic solutions to solubility, polarity, and band gap tuning. A considerable increase in the short circuit current density (I_{sc}) and PCE can be observed in **P2** and **P3** relative to **P0** and **P1** (Figure 3a). The results are shown for the 1:4 blend ratio (for cell performance dependence on blend ratio for **P2** and **P3**, see Figure 4). The increase in the number of rings is also expected to result in an increase of the intrachain mobility because of more extended π-conjugation. Since a clear trend in the increase in the mobility is observed for the blend films (according to the results obtained by the space-charge-limited current (SCLC) modeling shown in Figure 5), it is likely that intrachain mobility significantly contributes to the bulk properties. Similar trends have been previously observed in monosilanylene−oligothienylene copolymers with different numbers of thienyl rings.[15d] Both **P2** and **P3** blended with PCBM exhibit carrier mobilities of the order of 10^{-4} cm^2 V^{-1} s^{-1} and have comparable photovoltaic efficiencies, although **P3** has a slightly higher absorption at longer wavelengths. This is likely due to the differences in film roughness and phase separation in **P2**:PCBM and **P3**:PCBM blends (for AFM images of 1:4 and 1:5 blends for both polymers, see Figure 6). From Figure 5, we note that the **P3**:PCBM blend can exhibit a reasonably balanced

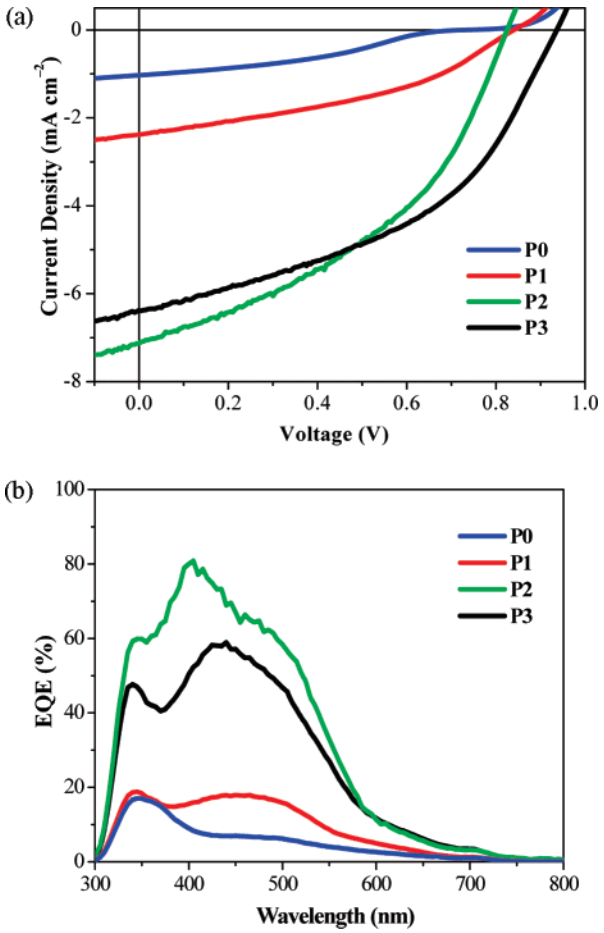

Figure 3. (a) *J*−*V* curves of solar cells with **P0**−**P3**:PCBM (1:4) active layers under simulated AM1.5 solar irradiation. (b) EQE wavelength dependencies of solar cells with **P0**−**P3**:PCBM (1:4) active layers.

charge transport, as required for efficient solar cell performance.[3i] The mobilities of the blends with **P0** and **P1** are somewhat lower, and we can observe that, for both electrons and holes, the mobilities increase with an increasing number of thienyl rings. Thus, not only optical but also charge transport properties can be tuned by changing the length of oligothienyl chains. As for the fill factor (FF), the relatively low values are at least partly due to the fact that all processing (except PEDOT:PSS annealing and electrode deposition) and measurements have been done in an ambient atmosphere which likely results in the presence of traps. We expect FF to improve for fabrication and characterization to be performed in an inert gas environment. A comprehensive study of charge transport and the influence of traps is necessary to further improve the fill factor and overall device performance. A high PCE of up to 2.50−2.66% can be obtained for **P2** and **P3** under illumination of an AM1.5 solar simulator, which can compete with that of P3HT-based devices

(15) (a) Garcia, P.; Pernaut, J. M.; Hapiot, P.; Wintgens, V.; Valat, P.; Garnier, F.; Delabouglise, D. *J. Phys. Chem.* **1993**, *97*, 513. (b) Jestin, I.; Frère, P.; Mercier, N.; Levillain, E.; Stievenard, D.; Roncali, J. *J. Am. Chem. Soc.* **1998**, *120*, 8150. (c) Diaz, A. F.; Crowley, J.; Bargon, J.; Gardini, G. P.; Torrance, J. B. *J. Electroanal. Chem.* **1981**, *121*, 355. (d) Harima, Y.; Kim, D.-H.; Tsutitori, Y.; Jiang, X.; Patil, R.; Ooyama, Y.; Ohshita, J.; Kunai, A. *Chem. Phys. Lett.* **2006**, *420*, 387.

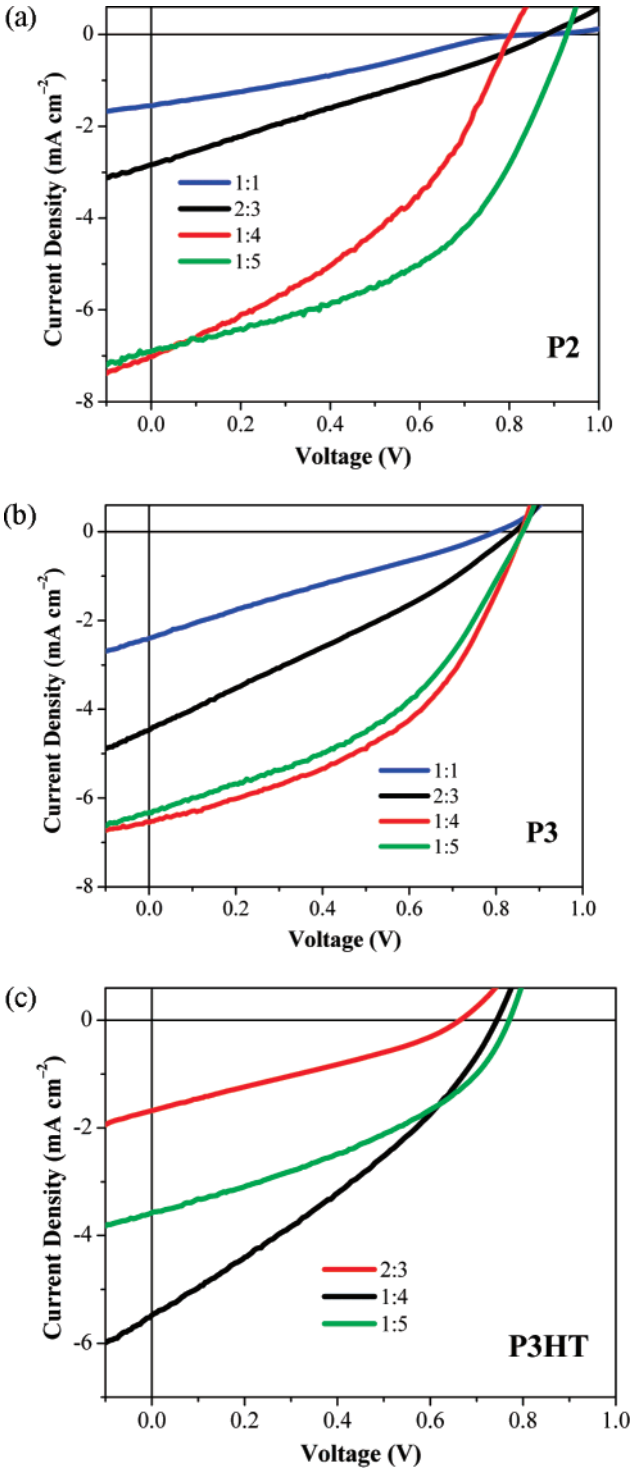

Figure 4. Effect of blend composition on solar cell performance. The curves shown are representative (close to average) curves from batches of 5−20 devices. (a) **P2**:PCBM, (b) **P3**:PCBM, and (c) P3HT:PCBM.

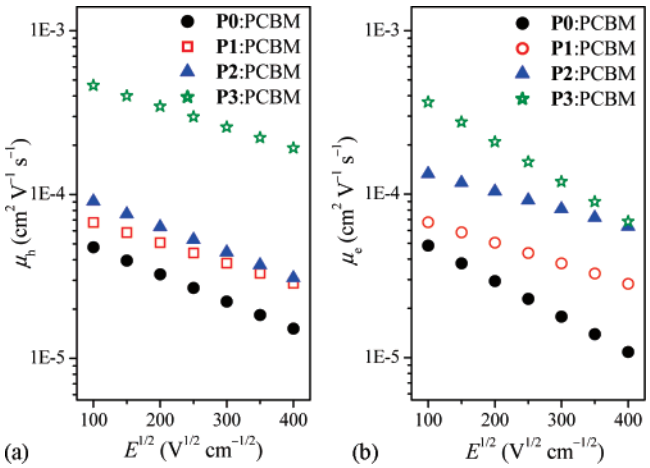

Figure 5. Comparison between (a) hole (μ_h) and (b) electron (μ_e) mobilities in **P0**−**P3**:PCBM blends obtained by the SCLC modeling.

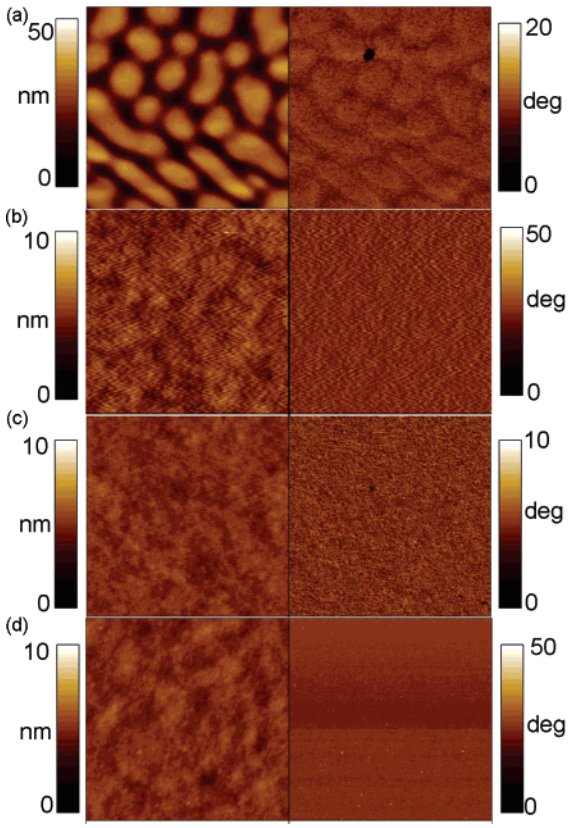

Figure 6. AFM topography (left) and phase contrast (right) images of blend films (a) **P2**:PCBM (1:4), (b) **P2**:PCBM (1:5), (c) **P3**:PCBM 1:4, and (d) **P3**:PCBM (1:5). Scan size is 1 μm × 1 μm.

fabricated without additional processing (annealing or TiO_x layer) both reported in the literature[3a] and obtained by us (see Supporting Information). The broad EQE curves for **P2** and **P3** cover almost the entire visible spectrum from 350 to 700 nm with a maximum of 81.3 and 59.3%, respectively (Figure 3b). Both the V_{oc} and *FF* values of **P2**- and **P3**-based solar cells (1:4) are quite close to each other. At the same blend ratio of 1:4, the PCE increases sharply from **P0** to **P3** (i.e., **P0** < **P1** < **P2** < **P3**), and it is remarkable to see that the light-harvesting ability of **P3** can be increased by ∼12 times relative to **P0** simply by adding more thienyl rings along the polymeric backbone. Yet, higher PCEs with excellent solution-processability are notoriously difficult to achieve with the pure organic polymers. Hence, the need to improve PCE to the practical level requires the implementation of new materials, and a new approach to capture sunlight for power generation involves putting metals into the conjugated organic polymers. The generally good solubility of platinum polyyne polymers over their purely organic poly(heteroaryleneethynylene)s favors the utilization of the metallopolyynes in the advance of polymer photovoltaic devices. The novel approach reported here can provide a useful avenue to PCE enhancement by extending the

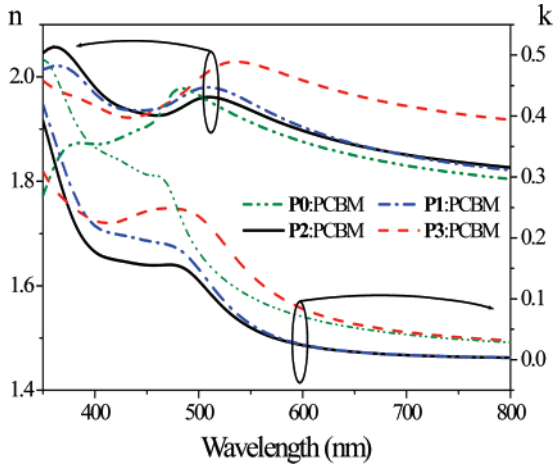

Figure 7. Real (n) and imaginary (k) parts of the refractive index of **P0**−**P3**:PCBM blend films. Ellipsometry measurements also confirm that **P3** has stronger absorption at longer wavelengths compared to polymers with a fewer number of thienyl rings.

absorption to longer wavelengths and metal incorporation without the involvement of the triplet excitons in the energy conversion which is recently believed to be a good way of making efficient polymer solar cells.[8f,h]

Generally, the amount of absorbed light depends not only on the cutoff absorption wavelength but also on the intensity of the absorption. A higher ϵ_{max} value of the polymer with a similar degree of polymerization would be anticipated as we increase *m*, and this can be exemplified by a gradual increase in ϵ_{max} from **M0** to **M3** (see Supporting Information), resulting in higher PCEs. To investigate in more detail the reasons for the excellent performance of **P2**:PCBM and **P3**:PCBM cells, we performed spectroscopic ellipsometry measurements of **P0**−**P3**:PCBM blend films. The obtained real and imaginary parts of the index of refraction are shown in Figure 7. It should be noted that the relationship between the real and imaginary parts of the index of refraction of blend films and the number of thienyl rings is not simple, so that further study of phase separation in the blends for different blend compositions combined with more complex sample modeling is needed to fully understand the optical properties of the blends. In addition, the effects of surface roughness have not been taken into account. However, ellipsometry measurements clearly confirm that **P3** has a stronger absorption at longer wavelengths compared to polymers with fewer numbers of thienyl rings, leading to improved absorption of the solar radiation (Figure 7). However, **P3**:PCBM blend film also exhibits a slightly higher refractive index, so that as compared to the **P2**:PCBM blend more light is reflected at the PEDOT:PSS/**P3**:PCBM interface, resulting in a smaller increase in the efficiency of **P3**:PCBM compared to **P2**:PCBM than that expected from the difference in absorption and charge transport properties. Differences in surface roughness and phase separation (domain sizes) in different blends also likely play a role and require further study. Therefore, the design of the low band gap polymers for photovoltaic applications should consider not only lowering the gap but also increasing the absorption coefficient of the polymer, as well as optimizing the morphology of the blend films. Intensely colored metalloorganic polymers thus represent a promising class of materials for opening up new opportunities in photovoltaic applications, provided that low band gap and efficient and balanced charge transport are achieved. The obtained results clearly demonstrate the potential of metalated conjugated polymers in the future design of stable photovoltaic devices for commercialization purpose. It is expected that optimization of device architecture will result in further improvements in the efficiency and that tunability of the energy levels of the polymers is expected to be an asset in the applicability of this class of materials to solar cells with different acceptors.

Conclusion

In conclusion, we have demonstrated a versatile avenue for the tuning of polymer photophysical and charge-transporting properties and PCE in solar cells via the variation of oligothienyl chain length in strongly absorbing polyplatinaynes with solubilizing bithiazole units, and we have prepared highly efficient solar cells with PCEs of up to 2.7% and peak EQE to 83%. Given the excellent solution-processability as well as performance advantage, this work has great potential for enhancing the light-to-electricity conversion efficiencies of polymer solar cells to a level of practical applications without the need for exploiting the triplet excited states in promoting an efficient photoinduced charge separation. While it may be a promising research endeavor to use platinum polyynes with accessible triplet states for polymer solar cells, these polymers usually absorb only in the blue-violet spectral region (i.e., with wide bandgaps), and consequently the efficiency was low due to low coverage of the solar spectrum (e.g., only 0.27% in PCE for the Pt polyyne with 2,5-diethynylthiophene spacer). In other words, the design of metallopolyynes should be focused on the development of not only phosphorescent polymeric materials but also the low band gap counterparts for high-efficiency photovoltaics. Our present work clearly sets out on an unexplored strategy toward an effective tuning of the solar cell efficiency and charge transport properties in metalated conjugated polymers for the future development of polymer-based solar power generation.

Experimental Section

General. Solvents were carefully dried and distilled from appropriate drying agents prior to use. Commercially available reagents were used without further purification unless otherwise stated. All reagents for the chemical syntheses were purchased from Aldrich or Acros Organics. PCBM and regioregular P3HT (M_w 20 000−50 000) were purchased from American Dyes. PEDOT:PSS (Baytron VPAI 4083) was purchased from H. C. Starck. Reactions and manipulations were carried out under an atmosphere of prepurified nitrogen using Schlenk techniques. All reactions were monitored by thin-layer chromatography (TLC) with Merck precoated glass plates. Flash column chromatography and preparative TLC were carried out using silica gel from Merck (230−400 mesh). Fast atom bombardment (FAB) mass spectra were recorded on a Finnigan MAT SSQ710 system. NMR spectra were measured in $CDCl_3$ on a Varian Inova 400 MHz FT-NMR spectrometer, and chemical shifts are quoted relative to tetramethylsilane for ^1H and ^{13}C nuclei and H_3PO_4 for ^{31}P nucleus.

Physical Measurements. UV/vis spectra were obtained on an HP-8453 diode array spectrophotometer. The solution emission spectra and lifetimes of the compounds were measured on a Photon Technology International (PTI) Fluorescence QuantaMaster Series QM1 spectrophotometer. The phosphorescence quantum yields were determined in degassed CH_2Cl_2 solutions at 293 K against quinine sulfate in 0.1 N

H_2SO_4 ($\Phi_P = 0.54$).[16] The decay curves were analyzed using a Marquardt-based nonlinear least-squares fitting routine and were shown to follow a single-exponential function in each case according to $I = I_0 + A \exp(-t/\tau)$. Electrochemical measurements were made using a Princeton Applied Research model 273A potentiostat. The cyclic voltammetry experiment of the polymer film was performed by casting the polymer on the glassy-carbon working electrode with a Pt wire as the reference electrode, at a scan rate of 100 mV s^{-1}. The solvent in all measurements was deoxygenated MeCN, and the supporting electrolyte was 0.1 M [^{n}Bu$_4$N][BF_4]. Ferrocene was added as an internal reference after each set of measurements, and all potentials are quoted relative to that of the ferrocene−ferrocenium couple (taken as $E_{1/2} = +0.27$ V relative to the reference electrode). The oxidation (E_{ox}) potentials and optical bandgaps (E_g) were used to determine the HOMO and LUMO energy levels using the equations $E_{HOMO} = -(E_{ox} + 4.8)$ eV and $E_{LUMO} = (E_{HOMO} + E_g)$ eV (versus the internal standard ferrocene value of −4.8 eV with respect to the vacuum level).[17] Thermal analyses were performed with the Perkin-Elmer TGA6 thermal analyzer.

Synthesis of Platinum Model Complexes M0−M3. All of them were synthesized following the dehydrohalogenating coupling between *trans*-[PtCl(Ph)(PEt_3)$_2$][18] and the corresponding diterminal alkynes. A typical procedure was given for **M0** starting from **L0**.

To a stirred mixture of **L0** (46.9 mg, 0.10 mmol) and *trans*-[PtPh(Cl)(PEt_3)$_2$] (109 mg, 0.20 mmol) in Et_3N (30 mL) and CH_2Cl_2 (30 mL) was added CuI (5.00 mg). The solution was stirred at room temperature under nitrogen over a period of 12 h, after which all volatile components were removed under vacuum. The crude product was taken up in dichloromethane and purified on preparative silica TLC plates with CH_2Cl_2/hexane (1:1, v/v) as eluent. The product **M0** was obtained as a yellow solid (107 mg, 72%). IR (KBr): ν(C≡C) 2083 cm^{-1}; ^{1}H NMR ($CDCl_3$): $\delta = 7.30-7.29$ (m, 4H, Ar), 6.98−6.94 (t, 4H, $J = 7.6$ Hz, Ar), 6.82−6.78 (t, 2H, $J = 7.6$ Hz, Ar), 2.81−2.77 (t, 4H, $J = 8.0$ Hz, alkyl), 1.74−1.70 (m, 28H, alkyl), 1.34−1.25 (m, 24H, alkyl), 1.12−1.04 (m, 36H, alkyl), 0.88−0.85 ppm (t, 6H, $J = 6.8$ Hz, alkyl); ^{13}C NMR ($CDCl_3$): $\delta = 157.30$, 155.58, 155.01, 139.00, 127.98, 127.38, 121.39, 120.95, 99.11 (Ar + C≡C), 31.91, 30.68, 29.85, 29.81, 29.70, 29.67, 29.35, 22.68, 14.11 (nonyl), 15.11, 8.00 ppm (Et); ^{31}P NMR ($CDCl_3$): $\delta = 11.38$ ppm ($^1J_{P-Pt} = 2627$ Hz); FAB-MS: *m/z*: 1483 (M^+). Anal. Calcd (%) for $C_{64}H_{108}N_2P_4Pt_2S_2$: C, 51.81; H, 7.34; N, 1.89. Found: C, 51.90; H, 7.23; N, 1.77.

M1: Red-brown solid. Yield: 73%. (Eluent: CH_2Cl_2/hexane (1:1, v/v)). IR (KBr): ν(C≡C) 2082 cm^{-1}; ^{1}H NMR ($CDCl_3$): $\delta = 7.31-7.30$ (d, 4H, $J = 6.8$ Hz, Ar), 6.98−6.95 (m, 6H, Ar), 6.82−6.79 (d, 4H, $J = 12.4$ Hz, Ar), 2.94−2.90 (t, 4H, $J = 7.8$ Hz, alkyl), 1.76−1.71 (m, 28H, alkyl), 1.41−1.26 (m, 24H, alkyl), 1.14−1.06 (m, 36H, alkyl), 0.88−0.85 (t, 6H, $J = 7.0$ Hz, alkyl); ^{13}C NMR ($CDCl_3$): $\delta = 156.82$, 155.68, 153.67, 138.99, 131.53, 129.05, 128.31, 127.37, 126.86, 124.06, 121.40, 101.87 (Ar + C≡C), 31.91, 30.55, 29.60, 29.58, 29.50, 29.47, 29.31, 22.67, 14.12 (nonyl), 15.11, 8.02 ppm (Et); ^{31}P NMR ($CDCl_3$): $\delta = 11.07$ ppm ($^1J_{P-Pt} = 2623$ Hz); FAB-MS: *m/z*: 1648 (M^+). Anal. Calcd (%) for $C_{72}H_{112}N_2P_4Pt_2S_4$: C, 52.48; H, 6.85; N, 1.70. Found: C, 52.30; H, 6.67; N, 1.62.

M2: Red solid. Yield: 63%. (Eluent: CH_2Cl_2/hexane (1:1, v/v)). IR (KBr): ν(C≡C) 2080 cm^{-1}; ^{1}H NMR ($CDCl_3$): $\delta = 7.32-7.30$ (d, 4H, $J = 6.8$ Hz, Ar), 7.06−7.04 (t, 4H, $J = 4.2$ Hz, Ar), 6.98−6.95 (m, 6H, Ar), 6.82−6.79 (d, 2H, $J = 14.4$ Hz, Ar), 6.76−6.75 (d, 2H, $J = 4.0$ Hz, Ar), 2.97−2.93 (t, 4H, $J = 7.8$ Hz, alkyl), 1.81−1.70 (m, 28H, alkyl), 1.42−1.34 (m, 24H, alkyl), 1.14−1.06 (m, 36H, alkyl), 0.88−0.85 ppm (t, 6H, $J = 7.0$ Hz, alkyl); ^{13}C NMR ($CDCl_3$): $\delta = 157.30$, 155.72, 154.36, 139.16, 139.00, 132.54, 130.69, 130.16, 127.98, 127.72, 127.37, 123.76, 123.58, 123.09, 121.39, 102.16 (Ar + C≡C), 31.90, 30.48, 29.55, 29.46, 29.42, 29.40, 29.31, 22.68, 14.12 (nonyl), 15.11, 8.03 ppm (Et); ^{31}P NMR ($CDCl_3$): $\delta = 11.11$ ppm ($^1J_{P-Pt} = 2626$ Hz); FAB-MS: *m/z*: 1812 (M^+). Anal. Calcd (%) for $C_{80}H_{116}N_2P_4Pt_2S_6$: C, 53.02; H, 6.45; N, 1.55. Found: C, 52.88; H, 6.35; N, 1.48.

M3: Dark red solid. Yield: 43% (Eluent: CH_2Cl_2/hexane (1:1, v/v)). IR (KBr): ν(C≡C) 2079 cm^{-1}; ^{1}H NMR ($CDCl_3$): $\delta = 7.31-7.29$ (d, 4H, $J = 7.6$ Hz, Ar), 7.11−7.07 (m, 6H, Ar), 7.01−6.95 (m, 8H, Ar), 6.82−6.79 (t, 2H, $J = 7.0$ Hz, Ar), 6.76−6.75 (d, 2H, $J = 5.6$ Hz, Ar), 2.98−2.94 (t, 4H, $J = 7.4$ Hz, alkyl), 1.79−1.71 (m, 28H, alkyl), 1.42−1.26 (m, 24H, alkyl), 1.13−1.05 (m, 36H, alkyl), 0.88−0.85 ppm (t, 6H, $J = 6.6$ Hz, alkyl); ^{13}C NMR ($CDCl_3$): $\delta = 157.48$, 155.76, 154.63, 139.02, 138.35, 137.70, 134.27, 132.84, 131.48, 129.95, 128.11, 127.71, 127.55, 127.38, 124.68, 123.77, 123.60, 123.31, 121.39, 102.18 (Ar and C≡C), 31.91, 30.50, 29.56, 29.47, 29.43, 29.33, 22.70, 14.14 (nonyl), 15.11, 8.03 ppm (Et); ^{31}P NMR ($CDCl_3$): $\delta = 11.10$ ppm ($^1J_{P-Pt} = 2625$ Hz); FAB-MS: *m/z*: 1976 (M^+); Anal. Calcd (%) for $C_{88}H_{120}N_2P_4Pt_2S_8$: C, 53.48; H, 6.12; N, 1.42. Found: C, 53.50; H, 6.02; N, 1.47.

Synthesis of Platinum Metallopolyynes P0−P3. The polymers were prepared by the dehydrohalogenative polycondensation between *trans*-[Pt(*n*-Bu_3P)$_2Cl_2$][19] and each of **L0**−**L3**. A typical procedure was given for **P0** starting from **L0**.

Polymerization was carried out by mixing **L0** (46.9 mg, 0.10 mmol), *trans*-[Pt(*n*-Bu_3P)$_2Cl_2$] (67.1 mg, 0.10 mmol), and CuI (3.00 mg) in Et_3N/CH_2Cl_2 (30 mL, 1:2, v/v). After stirring at room temperature overnight under nitrogen, the solution mixture was evaporated to dryness. The residue was redissolved in CH_2Cl_2 and filtered through a short silica column using the same eluent to remove ionic impurities and catalyst residues. After removal of the solvent, the crude product was purified by precipitation in CH_2Cl_2 from MeOH two times. Subsequent washing with hexane and drying *in vacuo* gave a yellow solid of **P0** (92.7 mg, 87%). IR (KBr): ν(C≡C) 2087 cm^{-1}; ^{1}H NMR ($CDCl_3$): $\delta = 2.78$ (br, s, 4H, alkyl), 2.08 (br, s, 16H, alkyl), 1.55−1.25 (m, 48H, alkyl), 0.91−0.85 ppm (m, 24H, alkyl); ^{31}P NMR ($CDCl_3$): $\delta = 5.04$ ppm ($^1J_{P-Pt} = 2324$ Hz). Anal. Calcd (%) for $(C_{52}H_{92}N_2P_2PtS_2)_n$: C, 58.56; H, 8.70; N, 2.63. Found: C, 58.46; H, 8.78; N, 2.47.

P1: Yellow solid. Yield: 79%. IR (KBr): ν(C≡C) 2085 cm^{-1}; ^{1}H NMR ($CDCl_3$): $\delta = 6.97-6.95$ (m, 2H, Ar), 6.79−6.78 (d, 2H, $J = 4.4$ Hz, Ar), 2.93−2.90 (t, 4H, $J = 7.2$ Hz, alkyl), 2.13−2.09 (m, 12H, alkyl), 1.76−1.72 (m, 4H, alkyl), 1.61−1.56 (m, 12H, alkyl), 1.52−1.45 (m, 12H, alkyl), 1.39−1.26 (m, 24H, alkyl), 1.00−0.92 (m, 18H, alkyl), 0.88−0.85 ppm (t, 6H, $J = 6.8$ Hz, alkyl); ^{31}P NMR ($CDCl_3$): $\delta = 4.49$ ppm ($^1J_{P-Pt} = 2320$ Hz). Anal. Calcd (%) for $(C_{60}H_{96}N_2P_2PtS_4)_n$: C, 58.56; H, 7.86; N, 2.28. Found: C, 58.62; H, 7.66; N, 2.10.

P2: Red-brown solid. Yield: 59%. IR (KBr): ν(C≡C) 2083 cm^{-1}; ^{1}H NMR ($CDCl_3$): $\delta = 7.05$ (br, s, 4H, Ar), 6.98−6.97 (d, 2H, $J = 2.8$ Hz, Ar), 6.75−6.74 (d, 2H, $J = 2.8$ Hz, Ar), 2.94 (br, s, 4H, alkyl), 2.10 (br, s, 12H, alkyl), 1.78 (br, s, 4H, alkyl), 1.60−1.25 (m, 48H, alkyl), 0.97−0.84 ppm (m, 24H, alkyl); ^{31}P NMR ($CDCl_3$): $\delta = 4.53$ ppm ($^1J_{P-Pt} = 2322$ Hz); Anal. Calcd (%) for $(C_{68}H_{100}N_2P_2PtS_6)_n$: C, 58.55; H, 7.23; N, 2.01. Found: C, 58.43; H, 7.12; N, 1.94.

P3: Dark brown solid. Yield: 41%. IR (KBr): ν(C≡C) 2083 cm^{-1}; ^{1}H NMR ($CDCl_3$): $\delta = 7.13-7.09$ (m, 4H, Ar), 7.02−6.96 (m, 6H, Ar), 6.82−6.79 (t, 2H, $J = 6.0$ Hz, Ar), 2.95 (br, s, 4H, alkyl), 2.11 (br, s, 12H, alkyl), 1.79 (br, s, 4H, alkyl), 1.57−1.30 (m, 48H, alkyl), 0.98−0.84 ppm (m, 24H, alkyl); ^{31}P NMR ($CDCl_3$): $\delta = 4.50$ ppm ($^1J_{P-Pt} = 2319$ Hz). Anal. Calcd (%) for $(C_{76}H_{104}N_2P_2PtS_8)_n$: C, 58.55; H, 6.72; N, 1.80. Found: C, 58.34; H, 6.79; N, 1.67.

Solar Cell Fabrication and Characterization. The device structure was ITO/poly(3,4-ethylene-dioxythiophene):poly(styrene sulfonate) (PEDOT:PSS)/polymer:PCBM blend/Al. ITO glass substrates (10 Ω per square) were cleaned by sonication in toluene, acetone, ethanol, and deionized water, dried in an oven, and then cleaned with UV ozone

(16) Dawson, W. R.; Windsor, M. W. *J. Phys. Chem.* **1968**, *72*, 3251.
(17) (a) Thelakkat, M.; Schmidt, H.-W. *Adv. Mater.* **1998**, *10*, 219. (b) Ashraf, R. S.; Shahid, M.; Klemm, E.; Al-Ibrahim, M.; Sensfuss, S. *Macromol. Rapid Commun.* **2006**, *27*, 1454.
(18) Chatt, J.; Shaw, B. L. *J. Chem. Soc.* **1960**, 4020.
(19) Chatt, J.; Hayter, R. G. *J. Chem. Soc., Dalton Trans.* **1961**, 896.

for 300 s. As-received PEDOT:PSS solution was passed through the 0.45 μm filter and spin-coated on patterned ITO substrates at 5000 rpm for 3 min, followed by baking in N_2 at 150 °C for 15 min. The metallopolyyne:PCBM (1:4 by weight, unless specified otherwise) active layer was prepared by spin-coating the toluene solution (4 mg mL^{-1} of metallopolyyne, 16 mg mL^{-1} of PCBM) at 1000 rpm for 2 min. The substrates were dried at room temperature under low vacuum (vacuum oven) for 1 h and then stored under high vacuum (10^{-5}−10^{-6} Torr) overnight. An Al electrode (100 nm) was evaporated through a shadow mask to define the active area of the devices (2 mm circle). For comparison, solar cells with P3HT:PCBM active layers with different blend ratios were also prepared. The procedure for cell fabrication was the same, except that the P3HT:PCBM solution was prepared in chlorobenzene and stirred overnight in N_2 at 40 °C. All the fabrication procedures (except drying, PEDOT:PSS annealing, and Al deposition) and cell characterization were performed in air. Power conversion efficiency was determined from $J-V$ curve measurement (using a Keithley 2400 sourcemeter) under white light illumination (at 100 mW cm^{-2}). For white light efficiency measurements, an Oriel 66002 solar light simulator with an AM1.5 filter was used. The light intensity was measured by a Molectron Power Max 500D laser power meter. For the measurement of the external quantum efficiency, different wavelengths were selected with an Oriel Cornerstone 74000 monochromator, while the photocurrent was measured with a Keithley 2400 sourcemeter. The light intensity was measured with a Newport 1830-C optical power meter equipped with a 818-UV detector probe. AFM images have been obtained using Digital Instruments Nanoscope III AFM. The scan rate was 1.2 μm s^{-1}, and the tip force constant and resonant frequency were 0.7−0.9 N m^{-2} and 50−130 Hz, respectively. The charge carrier mobility was determined from the SCLC modeling.[20] The device structure was ITO/PEDOT:PSS/blend film/Au for the hole mobility determination, while for electron mobility determination the device configuration was ITO/Mg/blend film/LiF/Al. The mobilities were determined by fitting the measured $J-V$ curves to the SCLC model.[20] The index of refraction of the material was estimated from the modified Lorentz model fitting[21] of the ellipsometry data (obtained using JA Woollam V-VASE ellipsometer) for blend films spin-coated on Si substrates. Surface roughness correction was not used in the fitting. It should be noted that the surface roughness of **P2**:PCBM 1:4 blend films is significant, which may lead to underestimation of the extinction coefficient. Due to the lateral size of the surface features which is of the same order of magnitude as the wavelength, effective medium approximation is no longer applicable and the effect of the roughness cannot be taken into account. Thus, we have not used the surface roughness correction for all films to obtain a better comparison of the properties of the blends containing polymers with different numbers of thienyl rings. It should be noted that the roughness of the **P2**:PCBM 1:4 blend film in addition to the increased uncertainty in determined optical functions will also result in the increased absorption due to longer effective path length, in agreement with the measured higher absorbance for these films (see Supporting information). The mobility measurements for the **P0**:PCBM blend were also determined by the time-of-flight (TOF) technique for comparison. The samples for TOF measurements were prepared by drop-casting and then dried under vacuum, followed by the evaporation of a metal electrode in high vacuum (10^{-6} Torr). A nitrogen laser was used to generate pulsed excitation ($\lambda = 337.1$ nm). The transient photocurrent was monitored by an oscilloscope Tektronix TDS 3052B. The mobilities determined from TOF and SCLC were in good agreement, although the obtained values were slightly lower from the TOF measurements.

Acknowledgment. This work was supported by a CERG Grant from the Hong Kong Research Grants Council (HKBU 202607P) and a Faculty Research Grant from the Hong Kong Baptist University (FRG/06-07/II-63). K.-K. Chan acknowledges the receipt of a Prof. Sunney Chan Research Scholarship in 2007. Financial support from the Strategic Research Theme, University Development Fund, and Seed Funding Grant and Outstanding Young Researcher Award (administrated by The University of Hong Kong) is also acknowledged. We also thank S.-F. Cheung and Prof. K.-Y. Chan for AFM measurements. The authors also wish to thank Prof. Yong Cao of South China University of Technology, Guangzhou, China for his assistance in repeating photovoltaic measurements.

Supporting Information Available: Synthesis and characterization data of ligands, X-ray crystal structure of **L2-2Br** and crystallographic data for the reported structure (CIF format), absorption and emission spectra of **L0**−**L3** and **M0**−**M3**, solvent dependence of PL data for **P2** and **P3**, the $J-V$ curves of the solar cells in the dark as well as the charge carrier mobilities of **P0** as determined by both TOF and SCLC methods. This material is available free of charge via the Internet at http://pubs.acs.org.

JA074959Z

(20) Mihailetchi, V. D.; Xie, H.; de Boer, B.; Koster, L. J. A.; Blom, P. W. M. *Adv. Funct. Mater.* **2006**, *16*, 699.
(21) Liu, Z. T.; Kwok, H. S.; Djurišić, A. B. *J. Phys. D: Appl. Phys.* **2004**, *37*, 678.